Comparative reproductive biology of deep-sea ophiuroids inhabiting polymetallic-nodule fields in the Clarion-Clipperton Fracture Zone

Sven R Laming[1*], Magdalini Christodoulou[2], Pedro Martinez Arbizu[2], Ana Hilário[1]

[1]Centre for Environmental and Marine Studies (CESAM) & Department of Biology, University of Aveiro, 3810-193 Aveiro, Portugal

[2]German Centre for Marine Biodiversity Research (DZMB), Senckenberg am Meer, 26382 Wilhelmshaven, Germany

*** Correspondence:**
Corresponding Author
slaming@ua.pt

Keywords:

maturation, lecithotrophy, gonochoric, deep-sea mining, ecology, brittle stars, Ophiuroidea, Echinodermata

Abstract

Deep-sea mining in the Pacific Clarion-Clipperton Fracture Zone (CCZ), a low-energy sedimentary habitat with polymetallic nodules, is expected to have considerable and long-lasting environmental impact. The CCZ hosts extraordinarily high species diversity in nearly all domains of Life present. Data on species biology and ecology remain scarce, however. The current study describes the reproductive biology of *Ophiosphalma glabrum* (Lütken & Mortensen, 1899) (Ophiosphalmidae) and *Ophiacantha cosmica* (Lyman, 1878) (Ophiacanthidae), two ophiuroids frequently found in the CCZ. Specimens collected in Spring 2015 and 2019 in four contract areas (BGR, IOM, GSR, Ifremer) and one Area of Particular Interest (APEI 3) were examined morphologically and histologically. Size-class frequencies (disc diameter and oocytes feret diameters), sex ratios, gametogenic status, putative reproductive mode and a simple proxy for fecundity are presented. Habitat use differs in each. While *O. glabrum* is epibenthic, occurring as single individuals, *O. cosmica* often form size-stratified groups living on stalked sponges, suggesting gregarious settlement or retention of offspring (though no brooding individuals were found). Further molecular analyses are needed to establish whether *O. cosmica* groups are familial. In *O. glabrum*, for which sample sizes were larger, sex ratios approximated a 1:1 ratio with no size-structuring. In both species, individuals were at various stages of gametogenic maturity but no ripe females were identified. Based on this, *O. glabrum* is most probably gonochoric. Reproductive mode remains inconclusive for *O. cosmica*. Both species are presumptively lecithotrophic, with vitellogenic-oocyte feret diameters exceeding 250 µm. Oocyte feret diameters at times exceeded 400 µm in *O. glabrum*, indicating substantial yolk reserves. Estimates of instantaneous fecundity (vitellogenic specimens of *O. glabrum* only) were confounded by interindividual variability in gonad characteristics. The well-furnished lecithotrophic larvae of *O. glabrum* would be capable of dispersing even under food-impoverished conditions. The

current study examines ophiuroid reproductive biology over multiple localities in the CCZ concurrently for the first time, at sites characterised by differing productivity regimes. The reproductive biology of each species is thus discussed with reference to past evolutionary (habitat stability), contemporary (food supply) and future environmental drivers (potential impacts of deep-sea mining).

1 Introduction

The challenges of exploring remote deep-sea abyssal environments have, thus far, insulated the deep-sea benthos from the impacts of mineral resource extraction. However, the advent of the technological means to access and exploit the considerable mineral resources found in these environments (Ghosh and Mukhopadhyay, 2000), heralds imminent, unprecedented levels of disturbance in the deep-sea (Weaver et al., 2018). Faunae that have evolved under highly stable, food-limited environmental regimes are likely to be poorly adapted to large-scale disturbances that rapidly and/or irreversibly alter their environment (Stearns, 2000). The Clarion-Clipperton Fracture Zone (CCZ) in the tropical NE Pacific exemplifies this scenario, where the largest known global reserve of polymetallic nodules is located, formed over geological timescales in abyssal soft sediments characterized by very low sedimentation rates (Hein et al., 2013). Recent studies that have sought to describe the benthic fauna that typify the CCZ have also revealed extraordinarily high taxonomic diversity in nearly all domains of Life present (e.g. Amon et al., 2016; De Smet et al., 2017; Shulse et al., 2017; Wilson, 2017; Hauquier et al., 2018; Goineau and Gooday, 2019; Brix et al., 2020; Christodoulou et al., 2020), making the CCZ of critical importance for biodiversity conservation. In many of these studies, data (e.g. species-abundance curves) strongly suggest that many – arguably most – species remain unaccounted for, with high species turnover over relatively short spatial scales even in groups that are brooders like Isopoda (e.g. Wilson, 2017, Brix et al., 2020). Remoteness of habitat and spatial variability in species composition of this sort present challenges for performing robust ecological studies, as evidenced by the scarcity of ecologically meaningful data available for even the most conspicuous ‘common’ epifaunal species in the CCZ (Danovaro et al., 2017), including many echinoderm species (Amon et al., 2016).

Members of the phylum Echinodermata represent some of the most emblematic taxa found in deep-sea abyssal plains (Gage and Tyler, 1991). Echinoderms play a significant role in global marine carbon budget (Lebrato et al., 2010) and are abundant in many soft- and hard-substrate habitats globally (Gage and Tyler, 1991). The class Ophiuroidea are known to be particularly prevalent and diverse on bathyal slopes (e.g. O’Hara et al., 2008) but data concerning species diversity and abundances at abyssal depths are scarce by comparison (Stöhr et al., 2012). In the equatorial NE Pacific, such data is limited to select historic (e.g. HMS Challenger and Albatross expeditions, Lyman, 1878, 1879, 1882; Clark, 1911, 1949) and contemporary surveys (Amon et al., 2016; Vanreusel et al., 2016, Christodoulou et al., 2020). Drivers for large-scale regional variability in abyssal ophiuroid population densities are still poorly understood, however in the CCZ it seems that local-scale patchiness in nodule substrate availability plays a key role in determining the distribution of many species. Under certain habitat conditions, ophiuroids and the echinoderms more generally, comprise one of the largest components of mobile epifauna at nodule-rich sites (Amon et al., 2016; Vanreusel et al., 2016: up to 15 individuals per 100 m^2, with major contributions from ophiuroids). The presence of nodules appears particularly relevant to certain ophiuroid and echinoid species; when nodules are absent, mobile epifaunal densities fall sharply to one or two encounters in an equivalent 100 m^2 area, largely due to much-reduced encounters with ophiuroid species (Vanreusel et al., 2016). Two recent studies published in 2020, one based on video-transect surveys and the other on specimens collected by remotely operated vehicle (ROV) and epibenthic sledge (EBS), have also

identified ophiuroids in abundance and notably, at unexpectedly high levels of diversity in the easternmost regions of CCZ (Christodoulou et al., 2020; Simon-Lledó et al., 2020) with the discovery of previously unknown ancient lineages (Christodoulou et al., 2019, 2020).

Current knowledge of reproductive biology in abyssal ophiuroid species is limited to a few papers examining gametogenic and/or size-class patterns (e.g. *Ophiomusa lymani* in N Atlantic & NE Pacific, Gage, 1982; Gage and Tyler, 1982; *Ophiocten hastatum* in NE Atlantic, Gage et al., 2004; *Ophiura bathybia*, *Amphilepis patens*, *Amphiura carchara* and *O. cosmica* in NE Pacific, Booth et al., 2008; *Ophiura irrorata loveni*, *Ophiura lienosa*, *Amphioplus daleus*, *O. cosmica*, *Ophiernus quadrispinus* and *Ophioplexa condita* in S Indian Ocean, Billett et al., 2013), with no data available for specimens originating from polymetallic-nodule habitats. As part of a wider concerted effort to address significant knowledge gaps in our understanding of nodule-rich seabed ecology while this habitat remains relatively pristine, the current study describes the reproductive biology of the brittle stars *Ophiosphalma glabrum* Lütken & Mortensen, 1899 (Ophiosphalmidae) and *Ophiacantha cosmica* Lyman, 1878 (Ophiacanthidae), two of the more frequently encountered ophiuroids within the eastern CCZ (Christodoulou et al., 2020), based on histological analyses of specimens collected from several mining-contract areas within the eastern CCZ.

2 Methodology

2.1 Sample collection, fixation, preservation and species identification

Specimens were collected during remotely operated vehicle transects (ROV Kiel 6000, GEOMAR, manipulator arm) undertaken over the course of two cruises in Spring 2015 and 2019 on the R/V Sonne in the eastern CCZ. Cruise SO239 (11 March – 30 April 2015) visited four contract areas and one Area of Particular Environmental Interest (APEI, 400 x 400 square-km protected areas assigned to each of nine presumptive ecological subregions of the CCZ). The 2015 samples in the current study originated from three of these contract areas: BGR area (Federal Institute for Geosciences and Natural Resources, Germany); the southern IOM area (Interoceanmetal Joint Organization); and the easternmost GSR area (G-TEC Sea Mineral Resources NV, Belgium) as well as APEI 3, where each was located along a decreasing SE-to-NW particulate organic-flux (POC) gradient, concomitant with a decrease in surface primary productivity driven by basin-scale thermocline shoaling towards the N. Pacific subtropical gyre (Pennington et al., 2006). The 2019 samples from the follow-up cruise SO268 (18 Feb – 21 May), originated from BGR (again) and the central GSR contract area (2015-2019 site separation: BGR ~ 50 km; GSR ~ 350 km). A site map is provided in Figure 1.

Following collection, the arms of each specimen were removed for molecular analyses, while the central disc was fixed for reproductive histology. Arm fixation was in pre-cooled 96% EtOH, with replacement after 24 h (stored at -20 °C thereafter); disc fixation was in 4% phosphate-buffered formaldehyde (48 h) following by serial transfer to 70% ethanol, stored at room temperature. Specimens were later identified to species level based on morphological characteristics (*O. glabrum*: Lütken and Mortensen, 1899; Baker, 2016; *O. cosmica*: Lyman, 1878; Paterson, 1985), supported by mtDNA COI analyses of genomic DNA extracted from arm tissues, described in detail in Christodoulou et al. (2020).

2.2 Size measurements, dissection and tissue preparation for microscopy

Micrographs of the oral and aboral faces of central discs were created from focus-stacks taken under a stereomicroscope (Leica M125 and DMC5400 camera, LAS- Leica Application Suite 3.7; focus-stacking in Combine ZP 1.0). Disc diameter – the length from the radial shield's distal edge to the opposing interradial margin (Gage and Tyler, 1982) – was measured in LAS, to estimate size at first maturity and assess size-class frequencies as a function of sex. The aboral face, stomach and bursal-sac lining were then removed by dissection to reveal the bursal slits that border each arm base, along which the sac-like gonads are located, arranged in rows on each side. Intact gonad rows were dissected and then embedded either in paraffin wax or plastic resin, depending on tissue size. An additional decalcification step in 3% nitric acid in 70% ethanol (Wilkie, 2016) followed by a 70% ethanol rinse was required for smaller gonads, which were retained on a fragment of calcified tissue to facilitate tissue processing.

Larger gonad samples (all *O. glabrum* specimens and one *O. cosmica* specimen with larger gonads) were infiltrated in molten paraffin at 60 °C, following 6-step serial transfer to 100% ethanol, 4-step transfer to 100% MileGREEN™ (an iso-paraffin based solvent, Milestone) and final 2-step transfer to paraffin in a mould to set. Blocks were trimmed and 5-µm sections cut, relaxed in a water bath, placed on Superfrost™+ slides and dry-fixed by incubation at 50 °C. Slides were stained in (Harris') Haematoxylin & Eosin(-Y) following standard protocols with dehydration by replacement using ethanol. Note that the *O. cosmica* specimen processed using paraffin wax was also processed with LR white resin (protocol below) using neighbouring gonads, to identify any procedural biases in oocyte feret diameter.

Smaller tissue samples (all *O. cosmica* specimens) were blotted dry and then infiltrated directly in a hydrophilic methacrylate resin (LR white, London Resin Co.) at room temperature (3 resin replacements by micropipette, 30- mins. each, 4th overnight) then transferred to a fresh resin-filled gelatine capsule (size 00, Electron Microscopy Sciences, UK), which was capped and polymerised at 50 °C (20+ hrs). Having removed gelatine, LR-white resin pellets were trimmed and wet-sectioned on a Leica Ultracut UC6 Ultramicrotome (Germany), using a 45° glass knife. Sections 1-µm thick were transferred to individual aliquots arranged on Superfrost™+ slides. Periodic toluidine staining tracked progress through tissue. Standard H & E staining was modified by extending staining times and excluding ethanol, which distorts LR white. Slides were dried at 50 °C with a desiccant (see Laming et al., 2020 for details). Regardless of protocol, sections were then cleared in MileGREEN™ and mounted with a cover slip (Omnimount™, Electron Microscopy Sciences).

2.3 Gametogenic analyses

Stained serial sections were photographed under a compound microscope (Leica DM2500 with camera module ICC50W, LAS 3.7). Spermatogenesis was documented qualitatively only. Oogenesis was examined in more detail. Oocyte size frequencies were determined by image analysis of serial sections from ovaries, imported as image-stacks into Image-J (Schindelin et al., 2012) to track individual oocytes through the sample and prevent repeat counting. Up to 100 oocytes (with visible nuclei only) were counted per specimen, each measured along its longest axis (feret diameter) and classified into an oogenic developmental stage. Stages were: 1) *Previtellogenic* oocytes (Pv), smallest oocytes with no clear evidence of a germinal vesicle or vitellogenesis (i.e. eosinophilic granulated cytoplasm, rich in yolk proteins, has not yet developed); 2) *Vitellogenic I*, (VI) "early" vitellogenic oocytes that are less than twice the diameter of previtellogenic oocytes, with the beginnings of an eosinophilic cytoplasm and a distinct germinal vesicle; 3) *Vitellogenic II* (VII), "mid-stage" vitellogenic oocytes that clearly possess an eosinophilic granulated cytoplasm, but whose diameter is

less than double that of the germinal vesicle; 4) *Vitellogenic III* (VIII), "late" vitellogenic oocytes with large eosinophilic cytoplasmic reserves, whose diameter exceeds double that of the germinal vesicle; 5) *Asymmetric* (As), late vitellogenic oocytes with germinal vesicles located asymmetrically and in contact with the cell membrane, the precursor to germinal vesicle breakdown (GVBD) and onset of meiosis I; 6) *Polar bodies* (PB), oocytes that have undergone GVBD, with evidence of peripheral polar bodies, germinal vesicle lacking; and 7) *Mature* (M), fully mature oocytes, possessing only a small pronucleus.

Overall state of gonad maturity was assessed visually in terms of gonad aspect within the bursal sac and histological appearance. Gonad state was either defined as "immature" (no gonad), "no gametes" (gonad but no gametogenesis), "developing" (gametogenesis at all stages of development but with interstitial spaces remaining), "nearly ripe" (late-stage gametes dominate but gonad is not yet replete), "ripe" (fully mature gametes and no interstitial space) and "post-spawning / recovery" (some residual near-mature gametes remain alongside degraded material, epithelial and myoepithelial layers are thickened and nutritive phagocytes are typically present). For *O. glabrum*, the percentage area occupied by oocytes relative to gonad area and a maturity stage index (MSI) were also calculated, the latter using the 4th formula proposed from Doyle, Hamel and Mercier (2012): *Oocyte density x Size of individual*$^{-1}$ *x Oocyte surface area x 0.01*, where oocyte density in the current study refers to oocytes mm^{-2} of all gonads in cross section, size of individual^{-1} is reciprocal disc diameter in mm and oocyte surface area is calculated from the mean feret diameter ($\frac{1}{4}\pi d^2$).

2.4 Statistical analyses

Sex ratios for each species were assessed by χ^2 test. The statistical significance of rank-based differences was tested by Kruskal-Wallis H test for: 1) disc diameter as a function of sex (including a juvenile category); 2) oocyte feret diameter as a function of year, and of disc diameter (for a given visual gonad state) and; 3) percentage gonad occupied by oocytes, MSI and mean oocyte feret diameter each as a function of visual gonad state. Post-hoc pairwise comparisons were by Dunn test. To assess whether a trade-off exists between oocyte diameter and oocyte density (and thus, fecundity), a spearman rank-order correlation was used to assess the strength of any proportional relationship between oocyte density and mean oocyte feret diameter. N.B. expressions of variation around average values are standard deviation (sd., for means) and median absolute deviation (mad., for medians). All statistical and graphical analyses were performed in R 4.0.3 (R Core Team, 2020)[1], using packages *svglite*, *tidyverse*, *cowplot*, *ggExtra* and *ggpubr* (Attali and Baker, 2019; Wickham et al., 2019, 2020; Kassambara and Kassambara, 2020; Wilke, 2020), with figures prepared in Inkscape 1.0.2 (Inkscape Project)[2].

3 Results

3.1 Sex ratios, size-class frequencies and size at first maturation

A total of eighty *Ophiosphalma glabrum* individuals (26 in 2015, 54 in 2019) and twenty-three *Ophiacantha cosmica* individuals (8 in 2015, 15 in 2019) were processed. Of the two species, *Ophiosphalma glabrum* was larger (across entire sampling area, mean disc diameter 16.1 ± sd. 3.99 *vs*. *Ophiacantha cosmica* mean disc diameter 4.9 ± sd. 2.03, example specimens in Figure 2).

[1] https://www.R-project.org/

[2] https://inkscape.org

Diameters ranged from 5.7 – 25.2 mm in *O. glabrum* and 2.2 – 10.0 mm in *O. cosmica*. Although male *O. glabrum* specimens were numerically dominant (42 *vs.* 26 individuals), overall sex ratios did not differ significantly from a 1:1 ratio ($\chi^2_1 = 3.765$, $p > 0.05$). The three intermediate size classes for *O. glabrum* (together ranging from 12.5 – 20 µm) were characterised by equal numbers of males and females, however smaller and larger mature *O. glabrum* individuals outside these size classes were exclusively male (Figure 3). Ranked-disc diameters did not significantly differ between sexes in *O. glabrum*, only between mature (male/female) and immature specimens, resulting in significant global differences across the three categories when immature specimens were included in analyses (Kruskal-Wallis $\chi^2_2 = 32.20$, $p < 0.01$, Figure 3). Sample sizes were particularly small for specimens of *O. cosmica*, however due to an over-whelming dominance of females (7:1) sex ratios were found to be significantly different ($\chi^2_1 = 4.50$, $p < 0.05$). The only male *O. cosmica* collected was the largest individual of this species, making statistical comparisons of disc diameter between sexes impossible.

For both species, several immature specimens were retrieved (Figures 2 and 3), allowing rough estimates of size at first maturity to be made. In *O. glabrum*, the largest immature specimen (lacking discernible gonads) had an 11.93-mm wide disc; a further 11 smaller specimens also lacked gonads. The smallest *O. glabrum* individual that possessed a gonad was a male at 12.07 mm disc diameter, while the smallest female was 15.45 mm (gametogenesis observed in both), placing approximate sizes at first maturity in males at < 12 mm disc diameter and at < 15.5 mm disc diameter in females. In *O. cosmica*, size at first maturity is less concrete. The largest specimen with no discernible gonad had a disc diameter of 5.12 mm, with two smaller (4.28, 4.34 mm) and two larger (6.00, 7.04 mm) specimens each in possession of 1 – 2 very small gonad buds (ca. 100µm diameter) not yet furnished with gametes. The smallest individual in which gametogenesis was identified was a female of 4.96 mm with six larger females with disc diameters of 5.37 – 7.88 mm (Figure 3, select specimens in Figure 2). The largest individual – the only *O. cosmica* male – had a 9.98-mm wide disc.

3.2 Gonad state and gametogenesis

Gonad state and gametogenesis were assessed qualitatively in males (Figure 4, Supplementary figure 1) and both qualitatively and semi-quantitatively in females (Figures 4 and 5; Supplementary figures 1 and 2). No evidence of simultaneous hermaphroditism (i.e., ovotestes) were identified in either species. Most *O. glabrum* males' testes were *developing* (52 %) with easily identifiable cell chains – or spermatogenic columns – composed of progressively more-advanced stages of spermatogenesis, extending from the inner-sac membrane into the central lumen (Figure 4bi). Testes were somewhat angular (Figure 4di), lacking the creamy engorged appearance typical of ripe individuals (example in Figure 4dii). A further 33 % were considered *nearly ripe*, where testes aspect appears unchanged but spermatogenic columns are no longer clearly visible, with roughly equal proportions of central mature spermatozoa, and surrounding tightly packed cells at earlier stages of spermatogenesis. Three specimens were *ripe* (7 %), where gonads appear engorged, extensively spread throughout the bursal sac and replete with spermatozoa, which predominate (Figure 4bii, dii). Putative evidence of nutritive phagocytes was used as the basis for discriminating a minority of male specimens as being in a *post-spawn / recovery* state (7 %, Figure 4 biii, with gonad aspect in diii). The single *O. cosmica* male collected was at the *developing* stage, with evident spermatogenic columns (Supplementary figure 1a).

No *ripe* females were identified in either species. However, most *O. glabrum* females had ovaries in a *nearly ripe* state (53 % overall, 88 % in 2015, 39 % in 2019), where late-stage (VIII+) oocytes dominate but the ovary is not replete and has not yet spread far into the bursary sac (e.g. Figure 4aii,

cii). An equal proportion of individuals with ovaries *developing* and *post-spawn / recovery* (see Figure 4ai and aiii) were identified overall (23 % each) but this did not hold true by year (2015- one *developing* female representing 12 %; 2019- five *developing* and six *post-spawn / recovery* females representing 28 % and 38 % of specimens, respectively). All-but-one of the *O. cosmica* females were *developing* (e.g., Supplementary figure 1b). The smallest female was in a *post-spawn / recovery* state (or possibly *developing* for the first time).

The higher proportion of *nearly ripe O. glabrum* females in 2015 versus 2019, is reflected in significant differences in ranked oocyte feret diameters between 2015 and 2019 (Kruskal-Wallis χ^2_1 = 67.8, $p < 0.0001$). These differences, echoed by mean and median oocyte feret diameters for each year (2015- mean 159.5 ± sd. 91.4, median 149.5 ± mad. 109.0; and 2019- mean 112.0 ± sd. 78.3, median 88.0 ± mad. 57.8), relate to higher frequencies of VIII+ oocytes in the ovaries of specimens from 2015, clearly visible in the size-frequency data for both years (Figure 5bi). Unfortunately, low sample sizes prohibit the quantitative comparison of oocyte frequency distributions as a function of contract area, however the proportion of large, late-stage oocytes found in specimens at the eastern-most sites appears to be highest with an apparent decrease in large late-stage oocytes in areas further west (particularly in APEI 3, Figure 5bii). No significant differences in ranked oocyte feret diameters between the two sampling years was found for *O. cosmica* (Kruskal-Wallis χ^2_1 = 2.34, $p > 0.05$), which may reflect similar oocyte size-class means, medians and distribution profiles identified for this species in both years (2015- mean 82.3 ± sd. 40.7, median 79.1 ± mad. 43.7; and 2019- mean 94.4 ± sd. 40.0, median 90.8 ± mad. 39.3; profiles in Figure 5a), though very low sampling sizes are likely undermining the statistical power of the test. Maximum oocyte feret diameters for *O. glabrum* and *O. cosmica* were a mature oocyte of 453 µm and VIII oocyte of 273 µm, respectively. However, unlike *O. glabrum*, oocytes at stages more advanced than VIII were not observed in *O. cosmica* generally (Supplementary Figure 2a), so it is likely that maximum oocyte diameters in this species are underestimated.

In addition to classifying oogenic stage and measuring oocyte feret diameters, the cross-sectional area occupied by oocytes relative to gonad area (inner-sac membrane) was calculated for *O. glabrum* – where tissue section quality allowed – as a proxy for the degree to which female gonads were full. A maturity stage index (MSI) previously demonstrated to be more sensitive to subtle changes in gonad maturation (Doyle et al., 2012), was also calculated for *O. glabrum*. Percentage of gonad occupied by oocytes (Kruskal-Wallis χ^2_2 = 11.37, $p < 0.01$), mean oocyte feret diameter (Kruskal-Wallis χ^2_2 = 10.55, $p < 0.01$) and MSI (Kruskal-Wallis χ^2_2 = 9.13, $p < 0.05$) all differed significantly as a function of *O. glabrum* gonad state (Figure 6). Evident differences existed in MSI and in the relative gonad area occupied by oocytes in *nearly ripe* females, however these metrics both failed to resolve differences between *developing* and *post-spawn* females, with post-hoc pairwise comparisons revealing significant group differences only between *nearly ripe* females and the two other gonad states (Figure 6). Group differences in mean oocyte feret diameter were restricted to *nearly ripe* females and those classified as *post-spawn / recovery* (Figure 6), reflecting similar (non-significant) mean feret diameters between *developing* and *nearly ripe O. glabrum* females. Spearman-rank correlative analysis revealed oocyte density mm^{-2} of gonad cross-sectional area to be significantly, inversely related to mean oocyte feret diameter (coefficient $R = -0.74$, $p < 0.0001$) indicating a trade-off between energy investment per oocyte and the number of oocytes that can be produced.

Finally, intraindividual variation in the number and size of ovaries and oocyte densities per ovary in *O. glabrum* was considerable (examples in Figure 4). Several *developing* and *nearly ripe* females possessed neighbouring gonads at different stages of maturity both qualitatively and quantitatively, where differing proportions of late-stage (VIII+) oocytes resulted in median oocyte diameters with

large variances (Figure 7a). Not unexpectedly – since one directly informed the other – the proportion of oocytes at each stage of oogenesis was relatively consistent in a given gonad state, irrespective of specimen size (Figure 7b). However, ranked oocyte feret diameters overall were significantly higher in the largest *nearly ripe* disc-diameter size class, (17.5 – <20 mm) when compared with smaller size classes (based on post-hoc comparisons of a highly significant Kruskal-Wallis test for this gonad state: Kruskal-Wallis $\chi^2_2 = 18.94$, $p < 0.0001$, Figure 7a), indicating that although the relative proportion of later-stage oocytes is similar, larger females possess larger oocytes at equivalent stages of oogenesis. Significant post-hoc differences in ranked oocyte across size classes were also identified in individuals in a state of *post-spawn / recovery*, however this was due rather to the relative dominance of previtellogenic oocytes in one individual from the intermediate size category for this gonad state (15 – <17.5 mm: Kruskal-Wallis $\chi^2_2 = 12.63$, $p < 0.01$, Figure 7a). No significant size-related differences were identified in the oocyte feret diameters of *developing* individuals of either species (Figure 7a).

As a result of intra- and interindividual variability in gonad maturity overall, a reliable measure of fecundity proved impossible. However, extrapolating from 25µm of tissue sectioned per individual, late-stage (VIII+) oocyte counts mm-sectioned^{-1} ovary $^{-1}$ ranged from 1.3 – 12.0 oocytes in *developing* females (n = 5), 5.0 – 30.0 oocytes mm-sectioned^{-1} ovary $^{-1}$ in *nearly ripe* females (n = 14) and 1.5 – 5.0 oocytes mm-sectioned^{-1} ovary $^{-1}$ in *post-spawn / recovery* females (n = 2).

4 Discussion

The current study provides new ecologically relevant reproductive data for two species of ophiuroid living in an oligotrophic, highly stable low-energy environment in the NE equatorial abyss which, due to the presence of polymetallic nodules, is under future threat from deep-sea mining activities (Weaver et al., 2018). The current study documents the reproductive biology of *Ophiosphalma glabrum* for the first time. Equal sex ratios for intermediate modal disc-diameter size classes and the absence of any simultaneous hermaphrodites both point to gonochorism in *O. glabrum*. Unfortunately, the manner (and possibly timing) of sampling may have created biases in the size classes of each sex. Large (and ripe) females (i.e., > 20-mm disc diameters) were conspicuously absent, suggesting either an unlikely upper limit on female disc diameter, or most probably, that large females were overlooked. This may simply be symptomatic of a patchy (or sex-specific) distribution of females, where large communal echinoderm aggregations in the soft-sediment abyss only really occur during the episodic arrival of labile organic matter to the seafloor (Kuhnz et al., 2014; Smith et al., 2018) or during aggregative spawning events (Mercier and Hamel, 2009). Alternatively, since stomach contents of dissected specimens indicate that *O. glabrum* is a deposit feeder and deposit-feeding ophiuroids are known to feed infaunally (e.g., Gielazyn et al., 1999), it's possible that larger females spend more time out of sight below the sediment's surface foraging for food to meet the nutritional demands of vitellogenesis, which are likely to be considerable, given both the size of mature oocytes and inherent food limitations.

Oocyte feret diameters frequently exceeding 300 µm in the current study (max 453 µm in a mature oocyte) are indicative of a lecithotrophic (non-feeding) larval mode with substantial yolk-protein and lipid reserves (Young, 2003). Although this places an upper limit on transport time relative to planktotrophy, lecithotrophy releases larvae of nutritional constraints that likely exist in food-impoverished transport environments. Planktotrophic (feeding) larvae, by contrast, would be confined to water masses with higher detrital input (Young et al., 1997). Lecithotrophy necessitates

greater energy investment per oocyte than in planktotrophy. This likely places constraints on fecundity in a food-limiting environment (Ramirez Llodra, 2002), as evidenced by the inverse relationship between oocyte densities and feret diameter in the current study. Ovaries in the current study, when *nearly ripe*, were classified as such based mainly on oogenic characteristics, since striking external indications of maturity were lacking in female specimens. Coloration was inconsistent and ovaries were not engorged, nor had they spread extensively into the bursal sac, as was witnessed in at least one ripe male. This indicates considerable scope remained for further reproductive investment in the females collected, under suitable environmental conditions. Without ripe females and intra- and interannual time-series sampling it is not possible to ascertain whether gametogenesis is seasonal (Tyler and Gage, 1980; Gage and Tyler, 1982) or aperiodic ('continuous'), though the presence of all oogenic stages in most specimens suggests aperiodic or semi-continuous spawning behaviour (Brogger et al., 2013). Oocyte size-class data also appear to suggest that slight differences exist between 2015 and 2019, with a higher proportion of females approaching maturity in 2015. This could reflect the slightly different timing of cruises, as no *post-spawn recovery* females were found in 2015 or site-related differences for each year since site locations were not the same. Further data are necessary to confirm this.

In an oligotrophic environment lacking strong seasonal fluctuations in POC flux, apparent aperiodic (or 'continuous') gametogenesis may arise in species that spawn 1) periodically, but histological studies fail to identify their cyclical nature (Mercier et al., 2007; Mercier and Hamel, 2008) or 2) opportunistically, occurring in rapid response to increased food supply related to episodic massive changes in surface productivity and as such, remain undetected (Mercier and Hamel, 2009). Coupled with lecithotrophy, aperiodic opportunistic spawning would be resource-driven, allowing a species to respond to fluctuating food availability by investing in gametogenesis only when suitable conditions arise (e.g., Booth et al., 2008). Responsive reproductive modes of this sort appear to be a feature of bathyal and abyssal ecosystems in the tropical NE Pacific (Kuhnz et al., 2014; Smith et al., 2018) where the influences of episodic disturbance events are of greater influence than seasonal changes in surface productivity. Further sampling could also establish whether apparent downward trends in the proportions of late-stage oocytes found in the female specimen from the oligotrophic APEI 3 (Vanreusel et al., 2016; Christodoulou et al., 2020) reflect a lag in maturation rate, energetic constraints on reproductive output or simply a sampling artefact.

Maximum sizes recorded for *O. glabrum* vary considerably in the literature but the largest attributed to this species is a 35 mm disc diameter (Clark, 1913), though there exists an *Ophiomusium multispinum* specimen – now synonymised with *O. glabrum* – with a 40-mm wide disc (Clark, 1911). In either case, the largest individual in the current study falls considerably short of these sizes, at 25.2 mm. Aside from some concerns around species assignation in historical samples and difficulties in collecting representative samples of species that occur at low densities in expansive and remote environments, these larger specimens also originate from shallower habitats (e.g. Cocos, Malpelo and Carnegie Ridge, Panama Basin, depths 800 – 3200 m, Clark, 1911, 1913), where greater food availability arriving from productive coastal systems (Pennington et al., 2006) could enable larger maximum sizes. Although smaller specimens were undoubtedly underrepresented, enough immature *O. glabrum* were collected to establish a rough size at first maturity of < 12 mm, around 30 - 35 % maximum size. Without knowledge of growth rates, the time taken to reach these sizes remains unknown, however if measures of growth (e.g. Gage et al., 2004) or temporal size-class frequency analyses can be compiled in future studies, this value could be easily converted to an estimate of age at first maturity, a highly relevant conservation metric for response to disturbance.

Sample sizes for the smaller species *Ophiacantha cosmica* limit any detailed interpretation of their reproductive biology. However, some data on size-class distributions and oocyte feret diameters already exist for this species from nodule-free habitats at Station M in the NE Pacific and around Crozet Island in the Southern Indian Ocean (Booth et al., 2008; Billett et al., 2013). Although sex ratios were significantly different in the current study, little stock can be placed in this result as the total number of mature specimens numbered less than ten and maximum disc diameters for both sexes are markedly lower than in the literature. Evidence from other studies indicate that sex ratios follow a 1:1 ratio when sampled in larger numbers (Billett et al., 2013), with maximum disc diameters of 11 – 12 mm (Booth et al., 2008; Billett et al., 2013; M Christodoulou, personal observations), although the holotype's disc diameter for this species is unaccountably large at 18 mm (Lyman, 1878). Maximum oocyte feret diameter in the current study (VIII oocyte at 273 µm) also appears to be underestimated, when compared with those of specimens from the Crozet plateau (Billett et al., 2013), which reached maximum feret diameters exceeding 500 µm, indicating lecithotrophy (or direct development, though no evidence of brooding has ever been recorded, Billett et al., 2013; this study). This is to be expected as females in the current study were relatively small by comparison and only in *developing* states, with no oocytes in the final stages of meiosis (i.e., asymmetric or later). The only individual classified as *post-spawn* / *recovery* was probably developing for the first time, particularly in light of its small disc diameter. Billet et al. (2013), much like the current study, found no evidence that *O. cosmica* were hermaphroditic, a condition known to occur in some species from this genus (e.g., *O. fraterna*, Tyler and Gage, 1982, identified at the time as *O. bidentata* but now revised, Martynov and Litvinova, 2008), with evidence instead that it was gonochoric. Our data though limited, support this viewpoint. Size at first maturity for *O. cosmica* was assessed in the current study but remains approximate at < 4.96-mm disc diameter (in females), due to ambiguity around two relatively large specimens (6 – 7 µm disc diameters) that possessed tiny bud-like gonads in which no evidence for gametogenesis could be found. These gonads did possess nodes in which cell clumps with highly basophilic nuclei were located, which are believed to be gonadal precursors housing primordial germ cells (Supplementary figure 2c).

Ophiacantha cosmica has been recorded from various hard substrata and vertically elevated fauna, such as deep-sea corals (Tyler and Gage, 1980) and tube worms (Lauerman et al., 1996; Billett et al., 2013). In the current study, this species is recorded on stalked-sponge species *Caulophacus* sp. and *Hyalonema* spp for the first time. Although alternative hard substrates are available in the CCZ (most obviously, polymetallic nodules), *O cosmica* specimens here were exclusively epizoic; this species was not encountered elsewhere. Sponge stalks provide some of the most elevated fauna on the seafloor in the CCZ; colonising them at positions above the benthic boundary layer would mitigate the influences of sheer on current speeds, which likely aids in a suspension-feeding lifestyle (Booth et al., 2008). The specimens in the current study either occurred as single individuals or, in certain instances, as size-stratified groups (Supplementary figure 3), suggestive of gregarious behaviour, offspring retention or fissiparity (though pentameral *Ophiacantha* spp. are not known to be fissiparous, Lee et al., 2019). A more detailed molecular study would help to reveal common or distinct genetic origins for the members of these groups.

In contrast, deposit-feeding *O. glabrum* examined in the current study were epibenthic, as found in previous studies both within the CCZ (Amon et al., 2016; Glover et al., 2016; Christodoulou et al., 2020) and more generally in the NE Pacific (Booth et al., 2008). Single individuals generally occurred in the sediment around nodules, or under habitat forming fauna such as xenophyophores and non-stalked sponges.

The limited availability of food in the deep-sea soft-sediment benthos is a principal driver in structuring deep-sea benthic communities characterised by low population densities but high levels of diversity (Hardy et al., 2015). The CCZ is a vast, food-limited ecosystem, reliant on the arrival of particulate organic matter (POM) to the seafloor, dictated largely by productivity at the surface (Pennington et al., 2006). While nodule substrate availability plays a role in determining species distributions (Vanreusel et al., 2016), food availability – largely dependent on POM flux – will ultimately determine population densities. Having evolved under these relatively stable conditions, communities in the abyssal deep-sea may be poorly adapted and thus highly susceptible to future mining impacts. If, for example, elevated substrata provide a nursery-type habitat for *O. cosmica*, then the ramifications for reproductive success following future mining disturbance events are cause for concern. In addition, filter-feeding organisms are expected to be severely impacted by plumes and settling aggregates generated by the resuspension of sea-floor sediments during nodule collections, resulting in long-term loss of suspension feeding organisms (Simon-Lledó et al., 2019). As with all deposit feeders, changes in surface-sediment chemical and physical characteristics following mining activity (e.g., remobilisation of formerly sequestered heavy metals and sediment compaction) could increase the toxicity of ingested sediments and impact *O. glabrum*'s ability to forage for food.

Food availability (i.e., POC flux) in soft-sediment abyssal habitats is subject to spatial variability both regionally, due to an undulating seafloor topography and at ocean-basin scales, due its dependency on surface productivity (Smith et al., 2008). Such heterogeneity in POC flux could create habitat networks of richer or poorer food supply over spatial scales at which reproductive kinetics and larval dispersal become ecological relevant (Hardy et al., 2015). The CCZ lies along a POC flux gradient: lowest in regions that underlie central oligotrophic ocean gyres and highest beneath or adjacent to coastal and equatorial regions characterised by productive upwelling zones (Smith et al., 2008). Since population densities decrease concomitantly with POC flux (Tittensor et al., 2011), species in food impoverished areas often occur at densities below the minimum needed for reproductive success (e.g. critically low encounter rates for mating), rendering them wholly dependent on larval supply from populations in higher POC-flux habitats (the oligotrophic sink hypothesis, Hardy et al., 2015). The two species examined in the current study are relatively common in the CCZ and beyond (Booth et al., 2008; Amon et al., 2016; Christodoulou et al., 2019, 2020; Simon-Lledó et al., 2019). In fact, it is for this reason that the current reproductive study was even possible. However, the relative densities at which they occur at regional scales (such as between contract areas / APEIs) varies considerably (e.g. Christodoulou et al., 2020). Should mining activities proceed in regions of higher-POC flux that play a formative role as larval sources, this may have wide-reaching detrimental effects on the most food-limited populations of these and other species that employ planktonic larval dispersal.

Reproductive kinetics play a fundamental role in mediating biogeographic patterns, population dynamics, metapopulation connectivity and ultimately, species survival (Ramirez Llodra, 2002). While molecular approaches can be used to examine both historical and contemporary connectivity, the temporal resolution of these data remains too poor to discriminate between sporadic regional genetic exchange that then spreads locally over successive generations, and regular regional genetic exchange that acts to supplement local populations to a biologically meaningful degree. Reproductive ecology remains vital in bridging gaps in our understanding. The current study sought to add to the paucity of reproductive data for deep-sea species in nodule environments. It also highlights an uncomfortable truth in deep-sea ecology however: that classical reproductive studies of this sort, which necessitate large numbers of individuals, may not be practicable in habitats such as the CCZ where the most susceptible species are typically the rarest. Support for more ambitious approaches

that compensate for sampling constraints, such as temporal studies or permanent monitoring networks are urgently needed in order for conservation measures to be effective and informed.

5 Conflict of Interest

The authors declare that the research was conducted in the absence of any commercial or financial relationships that could be construed as a potential conflict of interest.

6 Author Contributions

AH conceived reproductive study. AH, MC and PMA coordinated sample collection, fixation and preservation. MC and PMA performed all aspects of molecular ID. SRL performed specimen imagery, dissections, sectioning, histological, graphical and statistical analyses, prepared figures and wrote manuscript with scientific input from remaining authors.

7 Funding

Cruises SO239 and SO268 were financed by the German Ministry of Education and Science (BMBF) as a contribution to the European project JPI Oceans “Ecological Aspects of Deep-Sea Mining”. PMA acknowledges funding from BMBF under contract 03F0707E and 03F0812E. SRL and AH are supported by FCT/MCTES through CESAM (UIDP/50017/2020 + UIDB/50017/2020) funded by national funds, through the project REDEEM (PTDC/BIA-BMA/2986102/SAICT/2017) funded by FEDER within the framework of COMPETE2020 - Programa Operacional Competitividade e Internacionalização (POCI) and by Portuguese funds through FCT in special support of the JPIO pilot action “Ecological aspects of deep-sea mining” and the project MiningImpact2 (JPI Mining 2017, ref. Mining2/0002/2017), program 3599-PPCDT, Ciências do Mar - Sistemas Oceânicos e do Mar Profundo.

8 Acknowledgments

We would like to acknowledge the captain and crew of the R/V Sonne and ROV Pilots for the Kiel 6000 (GEOMAR) and to the deep-sea scientists involved in cruise organisation as well as collection and processing of samples on board. Our thanks to António and Sandra Calado for the use of an ultramicrotome.

9 References

9.1 Peer-reviewed

Amon, D. J., Ziegler, A. F., Dahlgren, T. G., Glover, A. G., Goineau, A., Gooday, A. J., et al. (2016). Insights into the abundance and diversity of abyssal megafauna in a polymetallic-nodule region in the eastern Clarion-Clipperton Zone. *Scientific Reports* 6, 1–12.

Baker, A. N. (2016). An illustrated catalogue of type specimens of the bathyal brittlestar genera *Ophiomusium* Lyman and *Ophiosphalma* HL Clark (Echinodermata: Ophiuroidea). *Zootaxa* 4097, 1–40.

Billett, D. S. M., Bett, B. J., Evans, R., Cross, I., Tyler, P. A., and Wolff, G. A. (2013). The reproductive ecology of deep-sea ophiuroids around the Crozet plateau, Southern Indian

ocean, under contrasting productivity regimes. *Deep Sea Research Part II: Topical Studies in Oceanography* 92, 18–26. doi:10.1016/j.dsr2.2013.03.002.

Booth, J. A. T., Ruhl, H. A., Lovell, L. L., Bailey, D. M., and Smith, K. L. (2008). Size–frequency dynamics of NE Pacific abyssal ophiuroids (Echinodermata: Ophiuroidea). *Marine Biology* 154, 933–941. doi:10.1007/s00227-008-0982-3.

Brogger, M. I., Martinez, M. I., Zabala, S., and Penchaszadeh, P. E. (2013). Reproduction of Ophioplocus januarii (Echinodermata: Ophiuroidea): a continuous breeder in northern Patagonia, Argentina. *Aquatic Biology* 19, 275–285.

Brix, S., Osborn, K. J., Kaiser, S., Truskey, S. B., Schnurr, S. M., Brenke, N., et al. (2020). Adult life strategy affects distribution patterns in abyssal isopods–implications for conservation in Pacific nodule areas. Biogeosciences 17, 6163–6184.Christodoulou, M., O'Hara, T. D., Hugall, A. F., and Arbizu, P. M. (2019). Dark Ophiuroid Biodiversity in a Prospective Abyssal Mine Field. *Current Biology* 29, 3909-3912.e3. doi:10.1016/j.cub.2019.09.012.

Christodoulou, M., O'Hara, T., Hugall, A. F., Khodami, S., Rodrigues, C. F., Hilario, A., et al. (2020). Unexpected high abyssal ophiuroid diversity in polymetallic nodule fields of the northeast Pacific Ocean and implications for conservation. *Biogeosciences* 17, 1845–1876.

Clark, A. H. (1949). Ophiuroidea of the Hawaiian islands. *Bulletin of the Bernice P. Bishop Museum* 195, 3–133.

Clark, H. L. (1911). *North Pacific Ophiurans in the Collection of the United States National Museum*. US Government Printing Office.

Clark, H. L. (1913). *Echinoderms from Lower California, with descriptions of new species*. , ed. Allen J. A. (Joel Asaph) New York: American Museum of Natural History Available at: https://www.biodiversitylibrary.org/item/86424.

Danovaro, R., Aguzzi, J., Fanelli, E., Billett, D., Gjerde, K., Jamieson, A., et al. (2017). An ecosystem-based deep-ocean strategy. *Science* 355, 452–454.

De Smet, B., Pape, E., Riehl, T., Bonifácio, P., Colson, L., and Vanreusel, A. (2017). The community structure of deep-sea macrofauna associated with polymetallic nodules in the eastern part of the Clarion-Clipperton Fracture Zone. *Frontiers in Marine Science* 4, 103.

Doyle, G. M., Hamel, J.-F., and Mercier, A. (2012). A new quantitative analysis of ovarian development in echinoderms: the maturity stage index. *Marine biology* 159, 455–465.

Gage, J. D. (1982). Age structure in populations of the deep-sea brittle star *Ophiomusium lymani*: a regional comparison. *Deep Sea Research Part A. Oceanographic Research Papers* 29, 1565–1586. doi:10.1016/0198-0149(82)90044-9.

Gage, J. D., Anderson, R. M., Tyler, P. A., Chapman, R., and Dolan, E. (2004). Growth, reproduction and possible recruitment variability in the abyssal brittle star *Ophiocten hastatum* (Ophiuroidea: Echinodermata) in the NE Atlantic. *Deep Sea Research Part I: Oceanographic Research Papers* 51, 849–864. doi:10.1016/j.dsr.2004.01.007.

Gage, J. D., and Tyler, P. A. (1982). Growth and reproduction of the deep-sea brittlestar *Ophiomusium lymani* Wyville Thomson. *Oceanologica acta* 5, 73–83.

Gage, J. D., and Tyler, P. A. (1991). *Deep-sea biology: a natural history of organisms at the deep-sea floor*. Cambridge University Press.

Ghosh, A. K., and Mukhopadhyay, R. (2000). Mineral wealth of the ocean. *Rotterdam, The Netherlands: AA Balkema, Rotterdam* 260.

Gielazyn, M. L., Stancyk, S. E., and Piegorsch, W. W. (1999). Experimental evidence of subsurface feeding by the burrowing ophiuroid *Amphipholis gracillima* (Echinodermata). *Marine Ecology Progress Series* 184, 129–138.

Glover, A. G., Wiklund, H., Rabone, M., Amon, D. J., Smith, C. R., O'Hara, T., et al. (2016). Abyssal fauna of the UK-1 polymetallic nodule exploration claim, Clarion-Clipperton Zone, central Pacific Ocean: Echinodermata. *BDJ* 4, e7251. doi:10.3897/BDJ.4.e7251.

Goineau, A., and Gooday, A. J. (2019). Diversity and spatial patterns of foraminiferal assemblages in the eastern Clarion–Clipperton zone (abyssal eastern equatorial Pacific). *Deep Sea Research Part I: Oceanographic Research Papers* 149, 103036. doi:10.1016/j.dsr.2019.04.014.

Hardy, S. M., Smith, C. R., and Thurnherr, A. M. (2015). Can the source–sink hypothesis explain macrofaunal abundance patterns in the abyss? A modelling test. *Proceedings of the Royal Society B: Biological Sciences* 282, 20150193.

Hauquier, F., Macheriotou, L., Bezerra, T. N., Egho, G., Martínez Arbizu, P., Janssen, F., et al. (2018). Meiofaunal communities in the Clarion-Clipperton Zone: geographic distribution and link with environmental conditions. in.

Hein, J. R., Mizell, K., Koschinsky, A., and Conrad, T. A. (2013). Deep-ocean mineral deposits as a source of critical metals for high-and green-technology applications: Comparison with land-based resources. *Ore Geology Reviews* 51, 1–14.

Kuhnz, L. A., Ruhl, H. A., Huffard, C. L., and Smith, K. L. (2014). Rapid changes and long-term cycles in the benthic megafaunal community observed over 24 years in the abyssal northeast Pacific. *Progress in Oceanography* 124, 1–11. doi:10.1016/j.pocean.2014.04.007.

Laming, S. R., Hourdez, S., Cambon-Bonavita, M.-A., and Pradillon, F. (2020). Classical and computed tomographic anatomical analyses in a not-so-cryptic *Alviniconcha* species complex from hydrothermal vents in the SW Pacific. *Frontiers in Zoology* 17, 12. doi:10.1186/s12983-020-00357-x.

Lauerman, L. M. L., Kaufmann, R. S., and Smith, K. L. (1996). Distribution and abundance of epibenthic megafauna at a long time-series station in the abyssal northeast Pacific. *Deep Sea Research Part I: Oceanographic Research Papers* 43, 1075–1103. doi:10.1016/0967-0637(96)00045-3.

Lebrato, M., Iglesias-Rodríguez, D., Feely, R. A., Greeley, D., Jones, D. O. B., Suarez-Bosche, N., et al. (2010). Global contribution of echinoderms to the marine carbon cycle: CaCO3 budget and benthic compartments. *Ecological Monographs* 80, 441–467. doi:10.1890/09-0553.1.

Lee, T., Stöhr, S., Bae, Y. J., and Shin, S. (2019). A New Fissiparous Brittle Star, *Ophiacantha scissionis* sp. nov. (Echinodermata, Ophiuroidea, Ophiacanthida), from Jeju Island, Korea. *Zool Stud* 58, e8–e8. doi:10.6620/ZS.2019.58-08.

Lütken, C. F., and Mortensen, T. (1899). The Ophiuridae. *Memoirs of the Museum of Comparative Zoölogy* 23, 93–208.

Lyman, T. (1878). Ophiuridae and Astrophytidae of the exploring voyage og HMS "Challenger" under Prof. Sir Wyville Thomson FRS. Part I. *Bull. Mus. Comp. Zool. Harvard* 5, 65–158.

Lyman, T. (1879). Ophiuridae and Astrophytidae of the exploring voyage og HMS "Challenger" under Prof. Sir Wyville Thomson FRS. Part II. *Bull. Mus. Comp. Zool. Harvard* 6, 17–83.

Lyman, T. (1882). Report on the Ophiuroidea dredged by HMS Challenger during the years 1873-1876. *Report of the Scientific Results of the Voyage of HMS Challenger during 1873-1876, Zoology* 5, 1–386.

Martynov, A. V., and Litvinova, N. M. (2008). Deep-water Ophiuroidea of the northern Atlantic with descriptions of three species and taxonomic remarks on certain genera and species. Marine Biology research 4, 76–111.Mercier, A., and Hamel, J.-F. (2009). *Advances in marine biology: endogenous and exogenous control of gametogenesis and spawning in echinoderms*. Academic Press.

Mercier, A., Ycaza, R. H., and Hamel, J.-F. (2007). Long-term study of gamete release in a broadcast-spawning holothurian: predictable lunar and diel periodicities. *Marine Ecology Progress Series* 329, 179–189.

O'Hara, T. D., Rowden, A. A., and Williams, A. (2008). Cold-water coral habitats on seamounts: do they have a specialist fauna? *Diversity and Distributions* 14, 925–934. doi:10.1111/j.1472-4642.2008.00495.x.

Paterson, G. L. (1985). The deep-sea Ophiuroidea of the north Atlantic Ocean. *Bulletin of the British Museum (Natural History)* 49, 1–162.

Pennington, J. T., Mahoney, K. L., Kuwahara, V. S., Kolber, D. D., Calienes, R., and Chavez, F. P. (2006). Primary production in the eastern tropical Pacific: A review. *Progress in Oceanography* 69, 285–317. doi:10.1016/j.pocean.2006.03.012.

R Core Team (2020). *R: A Language and Environment for Statistical Computing*. Vienna, Austria: R Foundation for Statistical Computing Available at: https://www.R-project.org/.

Ramirez Llodra, E. (2002). Fecundity and life-history strategies in marine invertebrates. *Advances in Marine Biology* 43, 87–170. doi:10.1016/S0065-2881(02)43004-0.

Schindelin, J., Arganda-Carreras, I., Frise, E., Kaynig, V., Longair, M., Pietzsch, T., et al. (2012). Fiji: an open-source platform for biological-image analysis. *Nature Methods* 9, 676–682. doi:10.1038/nmeth.2019.

Shulse, C. N., Maillot, B., Smith, C. R., and Church, M. J. (2017). Polymetallic nodules, sediments, and deep waters in the equatorial North Pacific exhibit highly diverse and distinct bacterial,

archaeal, and microeukaryotic communities. *MicrobiologyOpen* 6, e00428. doi:10.1002/mbo3.428.

Simon-Lledó, E., Bett, B. J., Huvenne, V. A. I., Köser, K., Schoening, T., Greinert, J., et al. (2019). Biological effects 26 years after simulated deep-sea mining. *Scientific Reports* 9, 8040. doi:10.1038/s41598-019-44492-w.

Simon-Lledó, E., Pomee, C., Ahokava, A., Drazen, J. C., Leitner, A. B., Flynn, A., et al. (2020). Multi-scale variations in invertebrate and fish megafauna in the mid-eastern Clarion Clipperton Zone. *Progress in Oceanography* 187, 102405. doi:10.1016/j.pocean.2020.102405.

Smith, C. R., De Leo, F. C., Bernardino, A. F., Sweetman, A. K., and Arbizu, P. M. (2008). Abyssal food limitation, ecosystem structure and climate change. *Trends in Ecology & Evolution* 23, 518–528.

Smith, K. L., Ruhl, H. A., Huffard, C. L., Messié, M., and Kahru, M. (2018). Episodic organic carbon fluxes from surface ocean to abyssal depths during long-term monitoring in NE Pacific. *Proceedings of the National Academy of Sciences* 115, 12235–12240. doi:10.1073/pnas.1814559115.

Stearns, S. C. (2000). Life history evolution: successes, limitations, and prospects. *Naturwissenschaften* 87, 476–486.

Stöhr, S., O'Hara, T. D., and Thuy, B. (2012). Global diversity of brittle stars (Echinodermata: Ophiuroidea). *PLoS One* 7, e31940.

Tittensor, D. P., Rex, M. A., Stuart, C. T., McClain, C. R., and Smith, C. R. (2011). Species–energy relationships in deep-sea molluscs. *Biology Letters* 7, 718–722.

Tyler, P. A., and Gage, J. D. (1980). Reproduction and growth of the deep-sea brittlestar *Ophiura ljungmani* (Lyman). *Oceanologica acta* 3, 177–185.

Tyler, P. A., and Gage, J. D. (1982). The reproductive biology of *Ophiacantha bidentata* (Echinodermata: Ophiuroidea) from the Rockall Trough. *Journal of the Marine Biological Association of the United Kingdom* 62, 45–55. doi:10.1017/S0025315400020099.

Vanreusel, A., Hilario, A., Ribeiro, P. A., Menot, L., and Arbizu, P. M. (2016). Threatened by mining, polymetallic nodules are required to preserve abyssal epifauna. *Scientific Reports* 6, 26808. doi:10.1038/srep26808.

Weaver, P. P. E., Billett, D. S. M., and Van Dover, C. L. (2018). "Environmental Risks of Deep-sea Mining," in *Handbook on Marine Environment Protection : Science, Impacts and Sustainable Management*, eds. M. Salomon and T. Markus (Cham: Springer International Publishing), 215–245. Available at: https://doi.org/10.1007/978-3-319-60156-4_11.

Wickham, H., Averick, M., Bryan, J., Chang, W., McGowan, L. D., François, R., et al. (2019). Welcome to the Tidyverse. *Journal of Open Source Software* 4, 1686.

Wilkie, I. C. (2016). Functional Morphology of the Arm Spine Joint and Adjacent Structures of the Brittlestar *Ophiocomina nigra* (Echinodermata: Ophiuroidea). *PLOS ONE* 11, e0167533. doi:10.1371/journal.pone.0167533.

Wilson, G. D. F. (2017). Macrofauna abundance, species diversity and turnover at three sites in the Clipperton-Clarion Fracture Zone. *Marine Biodiversity* 47, 323–347. doi:10.1007/s12526-016-0609-8.

Young, C. M. (2003). "Reproduction, development and life-history traits," in *Ecosystems of the deep oceans*, ed. P. A. Tyler (Amsterdam: Elsevier), 381–426.

9.2 R software and package references (those not subject to peer review)

R Core Team (2020). *R: A Language and Environment for Statistical Computing*. Vienna, Austria: R Foundation for Statistical Computing. Available at: https://www.R-project.org/.

Attali, D., and Baker, C. (2019). *ggExtra: Add Marginal Histograms to "ggplot2", and More "ggplot2" Enhancements*. Available at: https://CRAN.R-project.org/package=ggExtra.

Kassambara, A., and Kassambara, M. A. (2020). *ggpubr: "ggplot2" Based Publication Ready Plots.* Available at: https://CRAN.R-project.org/package=ggpubr.

Wickham, H., Henry, L., Pedersen, T. L., Luciani, T. J., Decorde, M., and Lise, V. (2020). *svglite: An "SVG" Graphics Device.* Available at: https://CRAN.R-project.org/package=svglite.

Wilke, C. O. (2020). *cowplot: Streamlined Plot Theme and Plot Annotations for "ggplot2."* Available at: https://CRAN.R-project.org/package=cowplot.

10 Supplementary Material

The Supplementary Material for this article can be found in an accompanying PDF presentation entitled "Supplementary material.pdf".

11 Data Availability Statement

Disc diameter and oocyte feret diameter measurements used in this study can be made available upon request.

12 Figures

Figure 1 Map of eastern Clarion-Clipperton Fracture Zone (CCZ) with sampling details
Map depicts the eastern half of the Area within the CCZ. Large 400 x400 km square regions are APEIs that border numerous exploration contract areas in the centre (N.B. reserved areas are not

shown). The areas in which specimens were collected are identified along with site locations for each cruise.

Figure 2 Example discs of *O. cosmica* and *O. glabrum* specimens used in the current study
The aboral and oral faces of a subset of specimens encountered during the latter SO268 cruise in 2019 are pictured, representative of the size ranges encountered. Abbreviations: **Juv** *juvenile*; **Un** *undetermined sex* (see main text).

Figure 3 Size-class frequency distributions of *O. glabrum* and *O. cosmica* disc diameters
Frequency histograms are colour-coded by sex (including a 'No gonad' category for immature specimens and an "Inconclusive" category for specimens with gonads devoid of gametes). Main χ^2 statistics relate to test for deviation from a 1:1 sex ratio (M vs F only). Marginal box and whisker plots depict medians (vertical line), inter-quartile (box width) and 90% (whisker) ranges in disc diameter for each sex category. Proximate K-W χ^2 statistic and p-value in a) relate to Kruskal-Wallis test for ranked differences in disc diameter as a function of all sex categories in *O. glabrum*. Significant post-hoc pairwise comparisons (Dunn's tests) are those with no letter annotations in common. Size-classes for each species are the same for comparative purposes.

Figure 4 Gametogenesis and gonad development in *O. glabrum*
Gonads at various stages of development in *O. glabrum*, as follows: a) i) *developing* ovaries, ii) *nearly ripe* ovaries and iii) *post-spawn* / *recovery* ovaries; b) i) *developing* testes in which spermatogenic columns (**SC**) are evident (indicated with arrows), ii) *ripe* testes and iii) *post-spawn* / *recovery* testes; c) visual aspect of i) *developing* ovaries [corresponding to a-i], ii) *nearly ripe* ovaries [corresponding to a-ii] and iii) a single ovary viewed down the distal-proximal axis, where late-stage oocytes are located distally (foreground), having previously developed from the basal region where early-stage oocytes are visible beneath, and finally; d) visual aspect of i) *developing* testes [corresponding to c-i], ii) *ripe* testes [corresponding to c-ii] and iii) *post-spawn* / *recovery* testes [corresponding to c-iii]. White arrowheads in c-d indicate single ovaries, purple dotted lines are midlines of arm bases. Other abbreviations: **As** *Asymmetric oocytes*, **NPh** *Nutritive phagocytes*, **Pv** *Previtellogenic oocytes*, **R** *Residual oocytes*, **VI** *Vitellogenic I oocytes*, **VII** *Vitellogenic II oocytes*, **Sz** *Spermatazoa*, **VIII** *Vitellogenic III oocytes*. Examples of gametogenesis in *O. cosmica* may be found in Supplementary figure 2.

Figure 5 Oocyte size-class frequency distributions for *O. cosmica* females
Frequency histograms display the relative proportions of oocyte feret diameters measured for each species. Only oocytes with nuclei were considered. Colour coding relates to associated oogenic developmental stages, assessed on a case-by-case basis for each oocyte counted and measured. Data for a) *O. cosmica* and b) *O. glabrum* are separated by year (2015, upper row; 2019, lower row) with *O. glabrum* data split further into c) each contract area sampled in a given year. N = number of females, n= number of oocytes pooled from N females. Frequency histograms for each species with both years' data pooled, are available in Supplementary figure 2.

Figure 6 Reproductive metrics plotted as a function of gonad state and oocyte density
a) Percentage-gonad occupied by oocytes, b) overall mean feret diameter per individual and c) a maturity stage index (MSI) developed by Doyle, Hamel, and Mercier (2012) were each calculated and evaluated as a function of gonad state, using Kruskall-Wallis Chi-squared tests on ranked data, the results of which are included in the top right corners for each. Significant post-hoc pairwise comparisons (Dunn's tests) are those with no letter annotations in common. Depicted in d) is the Spearman rank-correlation analysis performed to identify any relationship between mean oocyte diameters and corresponding densities, with the resulting Rho statistic (R), p-value and 95-% confidence intervals displayed.

Figure 7 Variation in feret diameter in *O. glabrum* and *O. cosmica* with specimen size
Displayed are a) Box and whisker plots and b) scatterplots displaying variation in oocyte feret diameters as a function of binned and continuous disc-diameter data (respectively) for female specimens in each gonad state identified. Significant differences in oocyte feret diameter with size were assessed (where relevant) for each gonad state, using Kruskall-Wallis Chi-squared tests on ranked data. Significant post-hoc pairwise comparisons (Dunn's tests) are those with no letter annotations in common. *Box and whisker values for this class based on two measurements only.

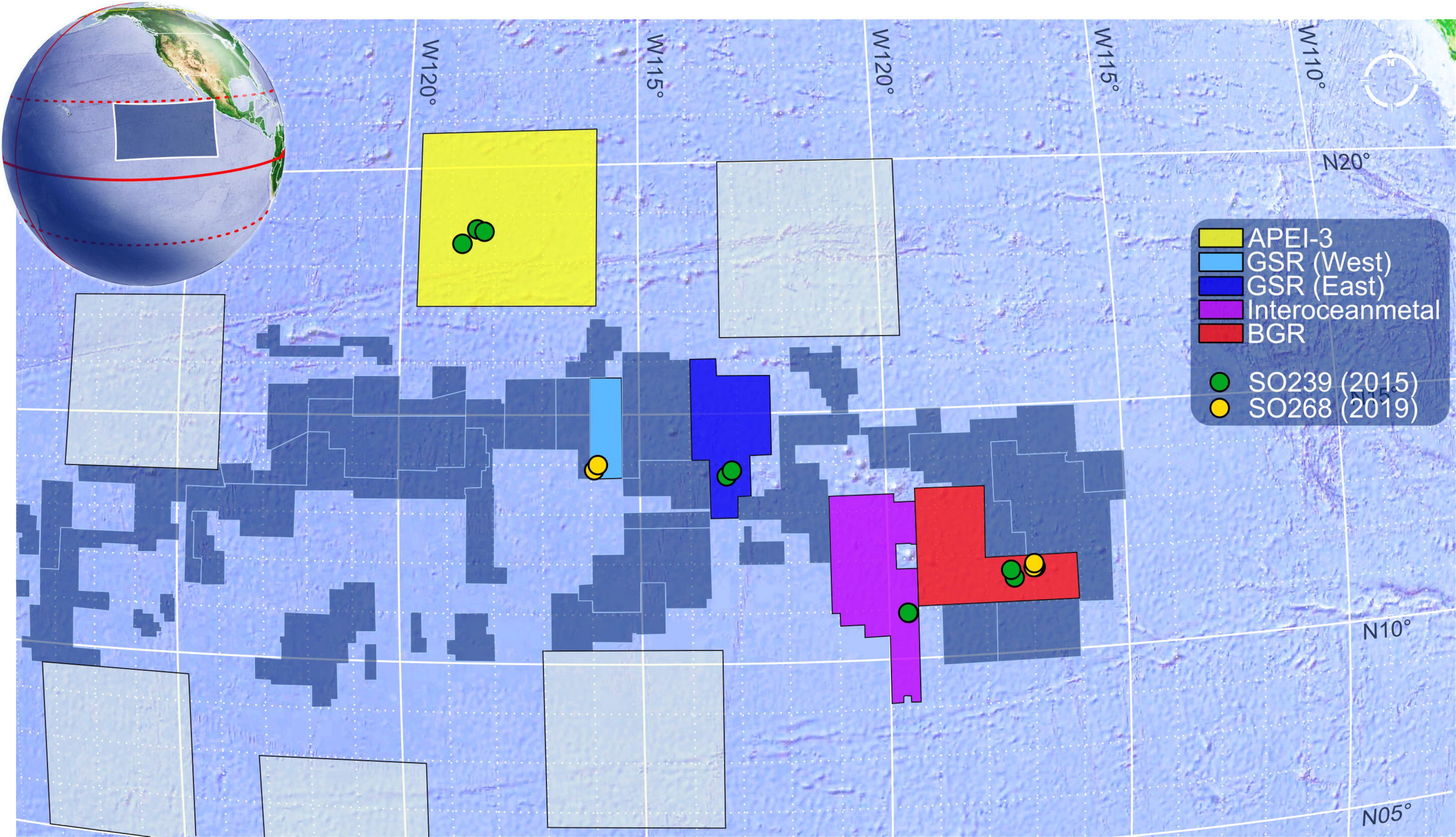
W120°
W115°
W120°
W115°
W110°
N20°
N10°
N05°
APEI-3
GSR (West)
GSR (East)
Interoceanmetal
BGR
SO239 (2015)
SO268 (2019)

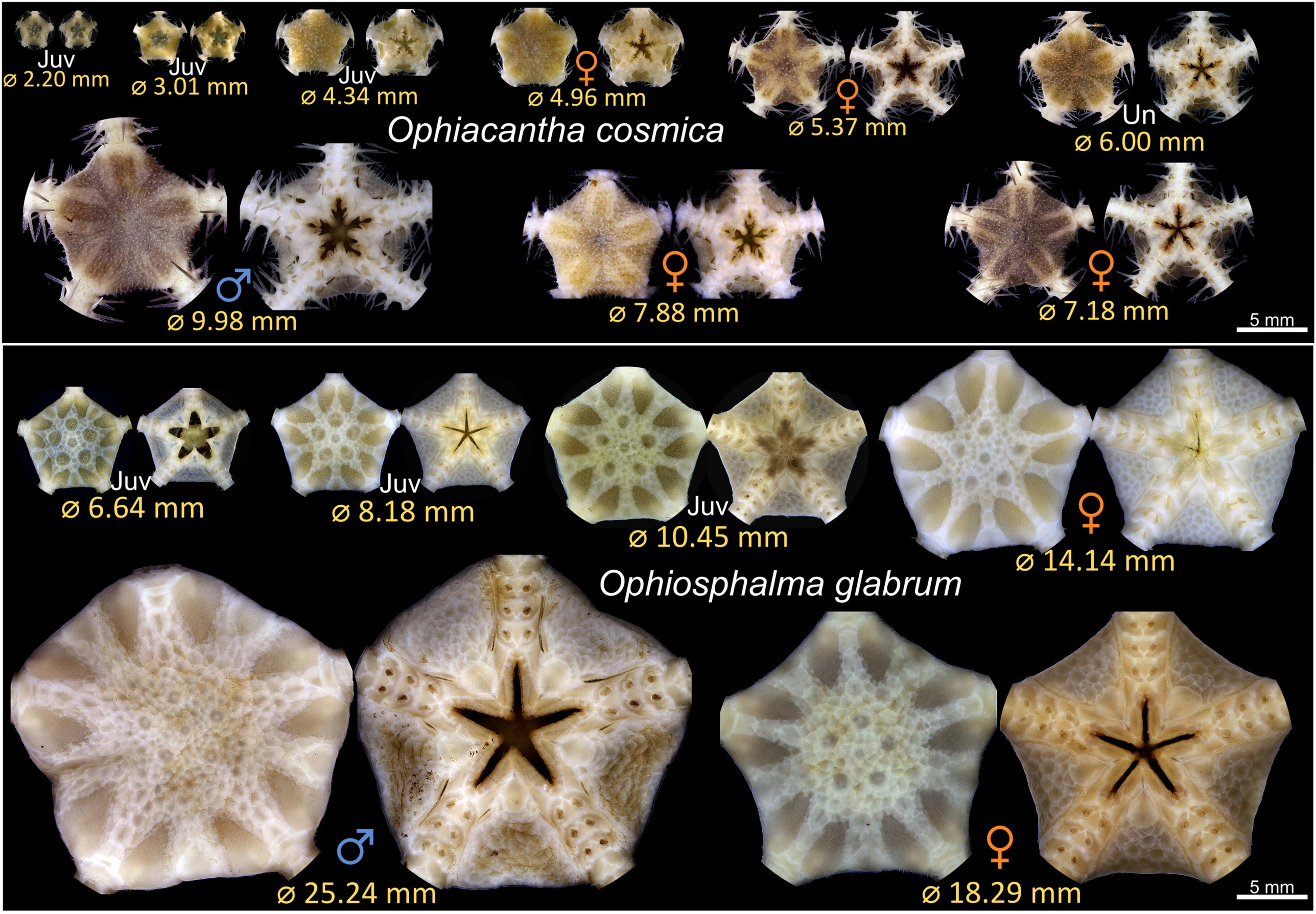
Juv
⌀ 2.20 mm
Juv
⌀ 3.01 mm
Juv
⌀ 4.34 mm
♀
⌀ 4.96 mm
Ophiacantha cosmica
♀
⌀ 5.37 mm
Un
⌀ 6.00 mm
♂
⌀ 9.98 mm
♀
⌀ 7.88 mm
♀
⌀ 7.18 mm
5 mm
Juv
⌀ 6.64 mm
Juv
⌀ 8.18 mm
Juv
⌀ 10.45 mm
♀
⌀ 14.14 mm
Ophiosphalma glabrum
♂
⌀ 25.24 mm
♀
⌀ 18.29 mm
5 mm

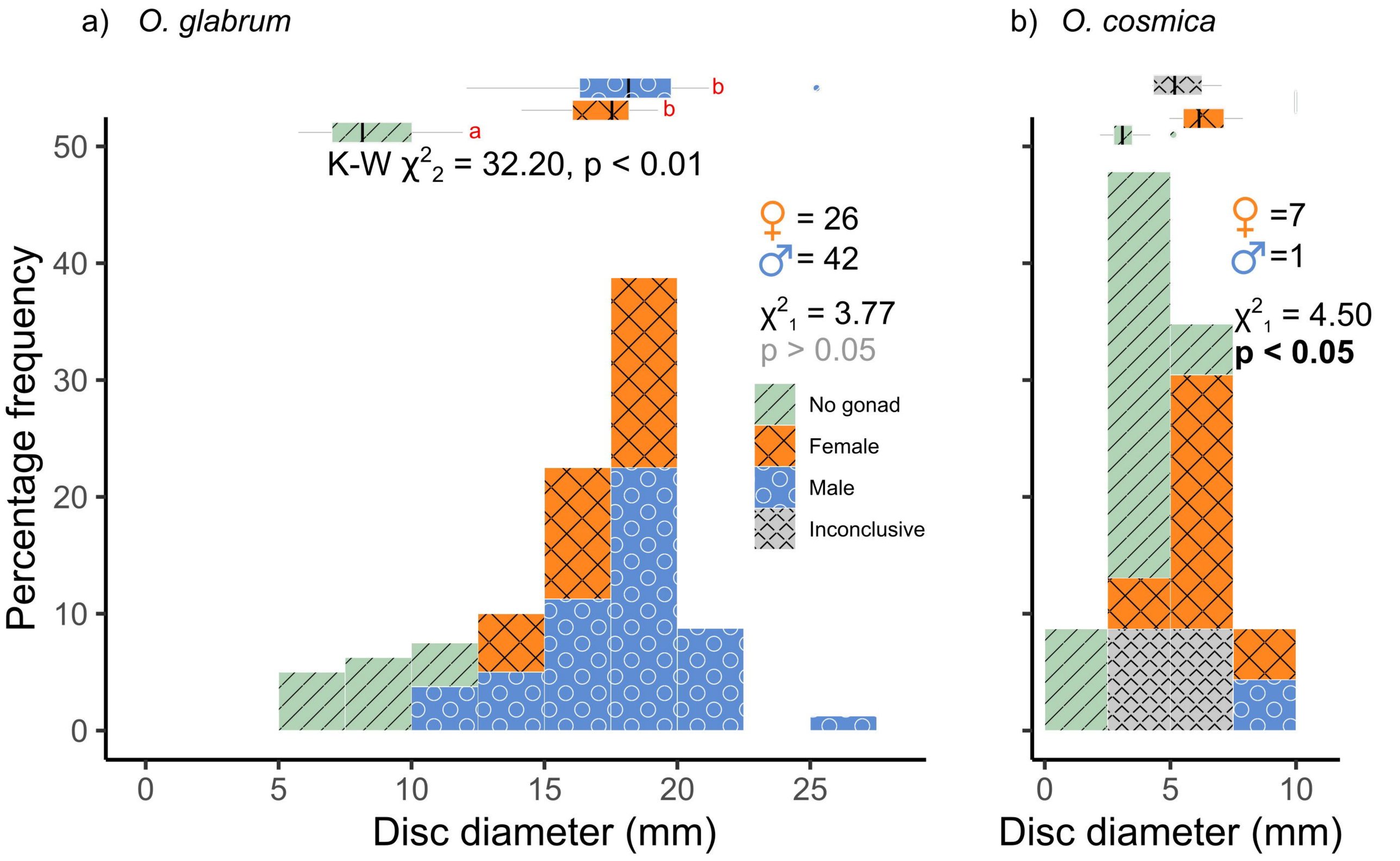
a) O. glabrum
b) O. cosmica
K-W χ^2_2 = 32.20, p < 0.01
a
b
b
♀ = 26
♂ = 42
χ^2_1 = 3.77
p > 0.05
No gonad
Female
Male
Inconclusive
♀ =7
♂ =1
χ^2_1 = 4.50
p < 0.05
Percentage frequency
0
10
20
30
40
50
0
5
10
15
20
25
Disc diameter (mm)
0
5
10
Disc diameter (mm)

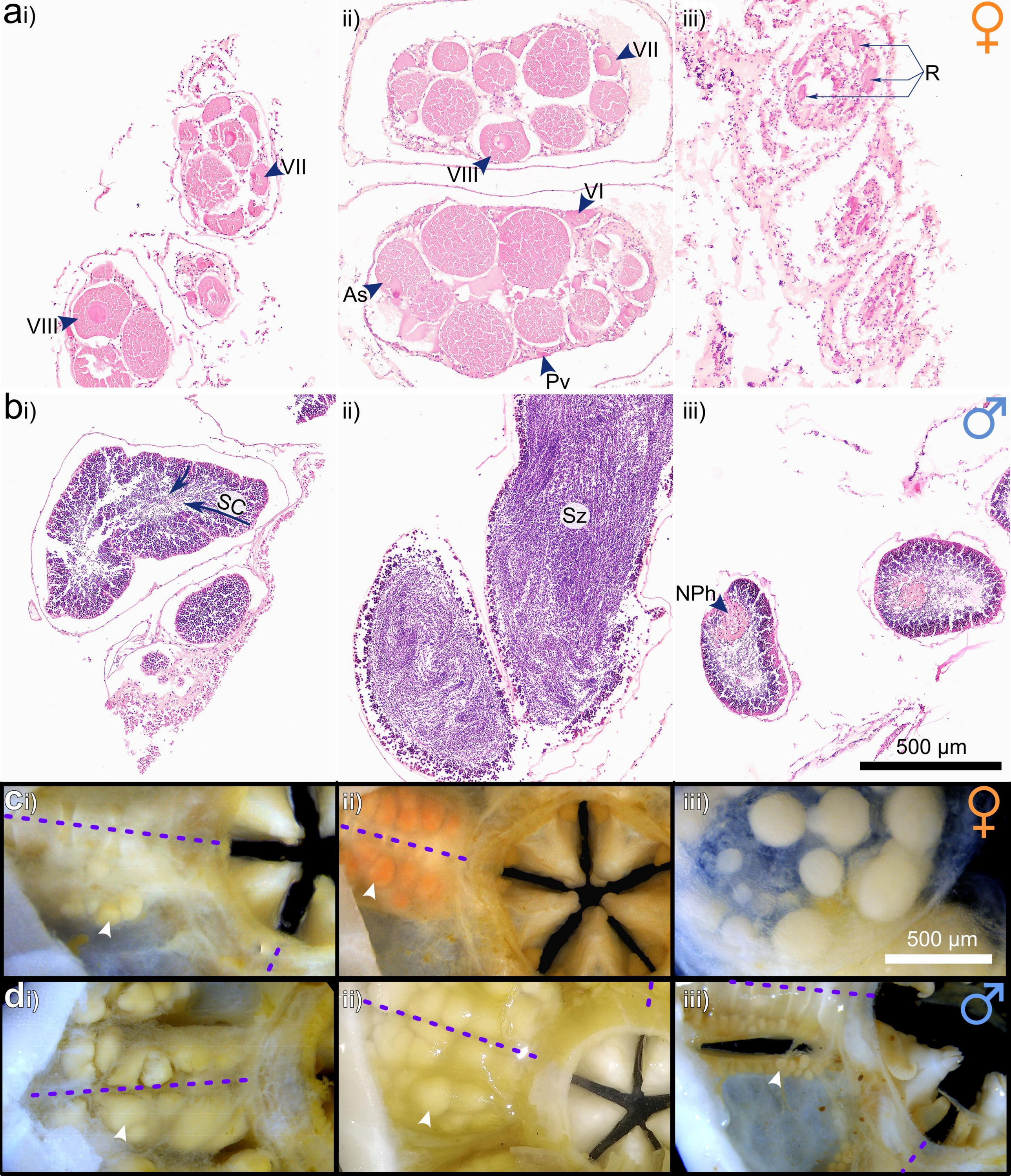
ai)
VII
VIII
ii)
VII
VIII
VI
As
Pv
iii)
R
bi)
SC
ii)
Sz
iii)
NPh
500 µm
ci)
ii)
iii)
500 µm
di)
ii)
iii)

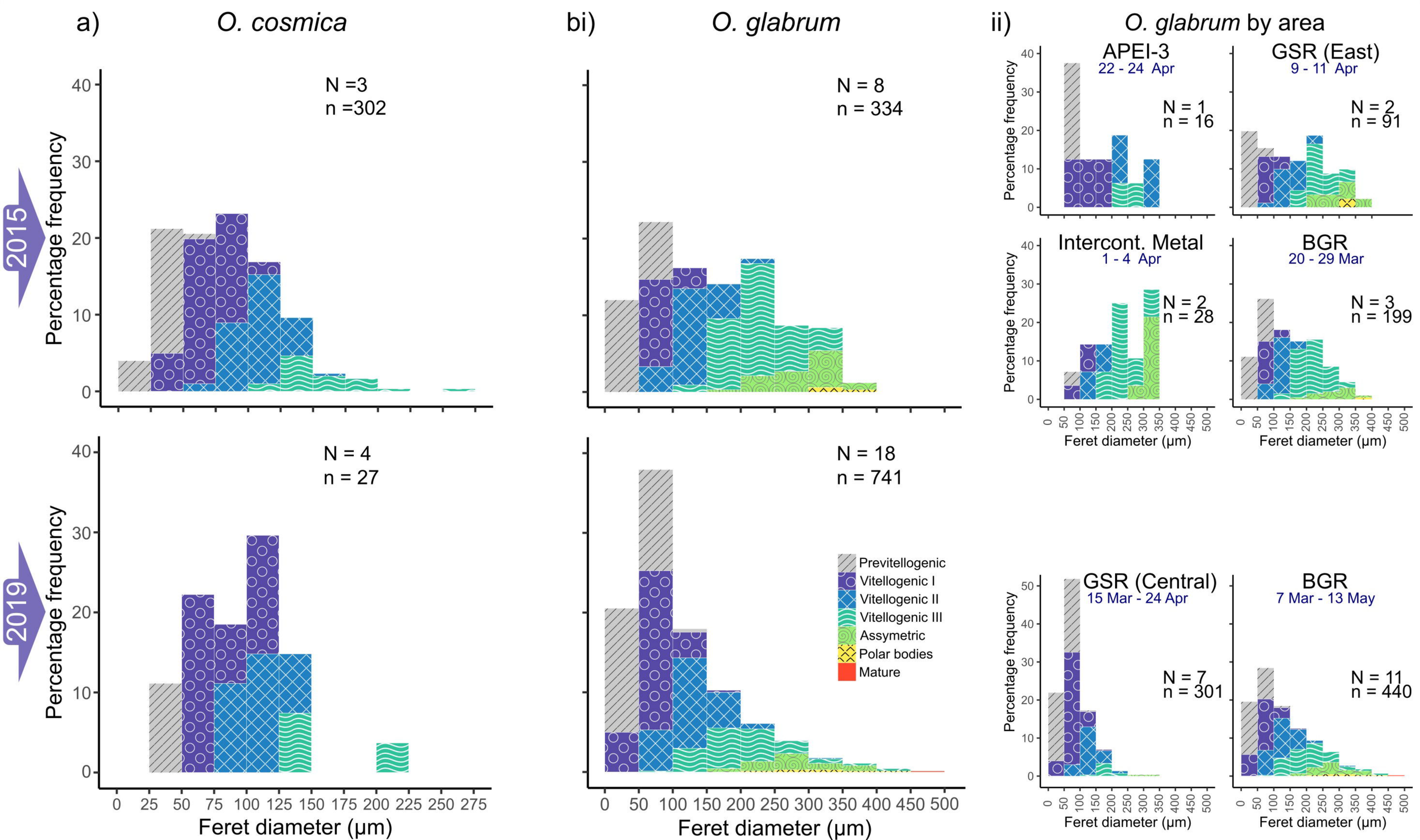
a)
O. cosmica
bi)
O. glabrum
ii)
O. glabrum by area
2015
2019
N =3
n =302
N = 8
n = 334
N = 4
n = 27
N = 18
n = 741
APEI-3
22 - 24 Apr
N = 1
n = 16
GSR (East)
9 - 11 Apr
N = 2
n = 91
Intercont. Metal
1 - 4 Apr
N = 2
n = 28
BGR
20 - 29 Mar
N = 3
n = 199
GSR (Central)
15 Mar - 24 Apr
N = 7
n = 301
BGR
7 Mar - 13 May
N = 11
n = 440
Previtellogenic
Vitellogenic I
Vitellogenic II
Vitellogenic III
Assymetric
Polar bodies
Mature
Percentage frequency
Feret diameter (µm)

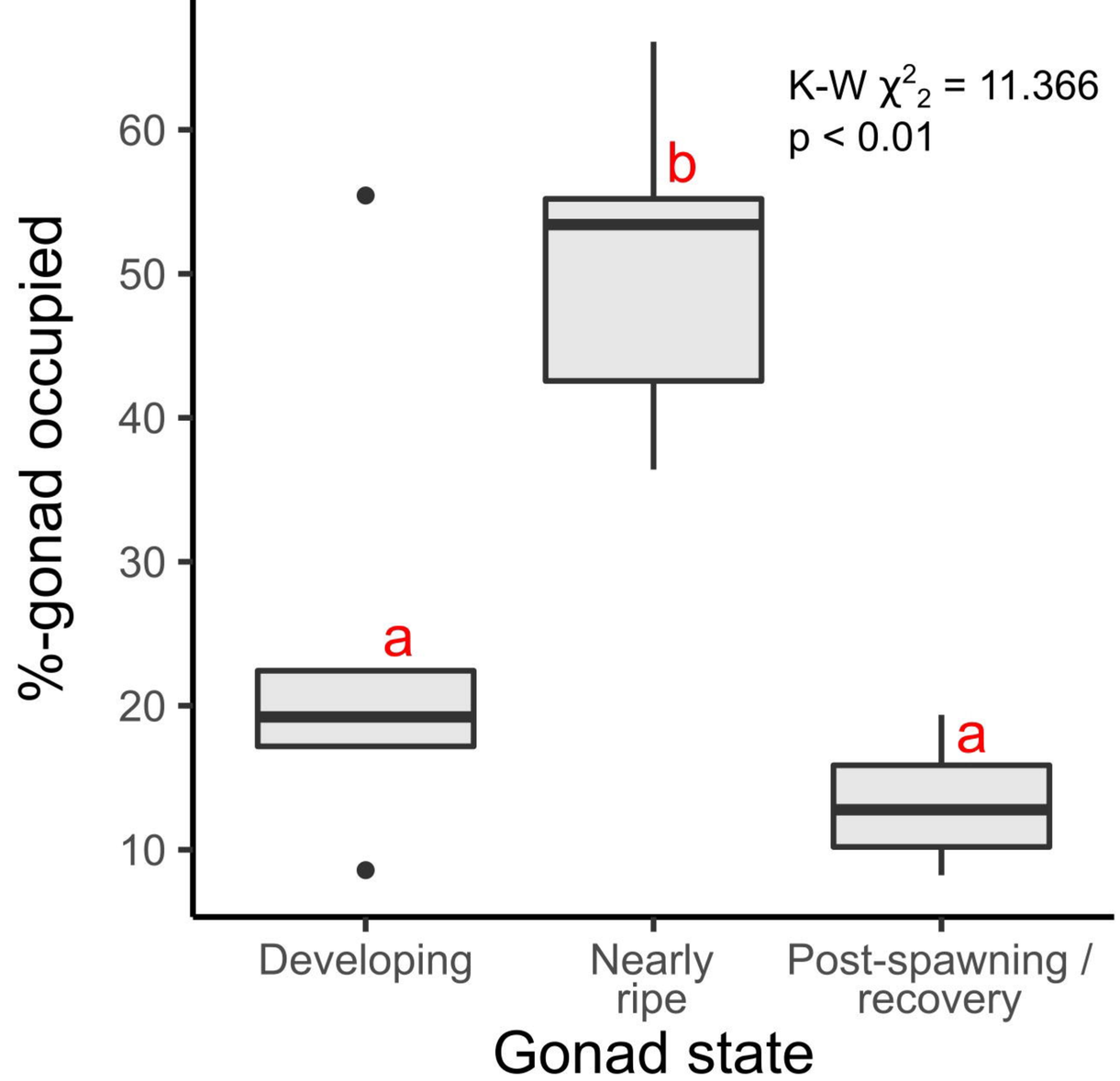
K-W χ^2_2 = 11.366
p < 0.01
%-gonad occupied
60
50
40
30
20
10
a
b
a
Developing
Nearly ripe
Post-spawning / recovery
Gonad state

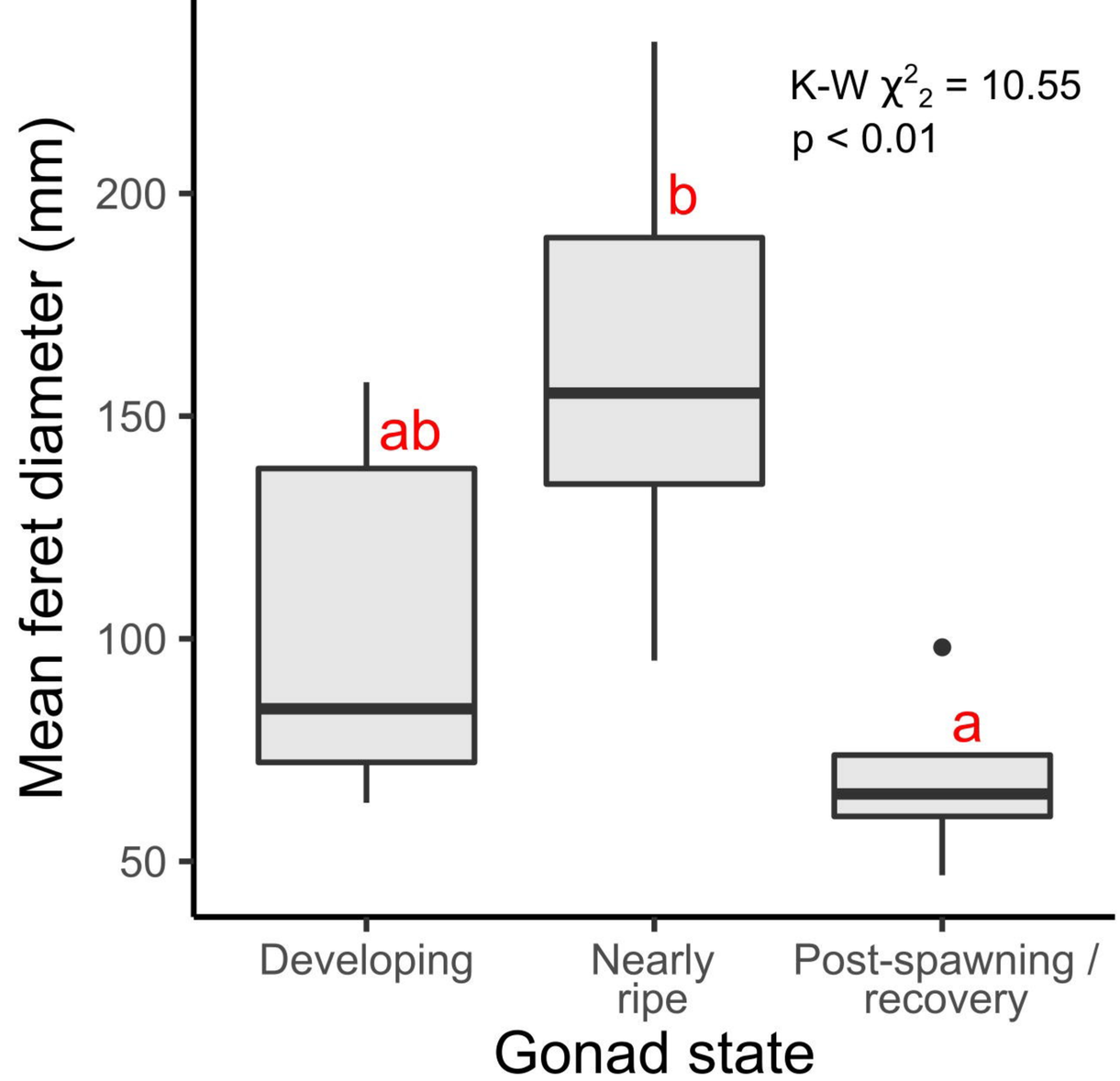
K-W χ^2_2 = 10.55
p < 0.01
Mean feret diameter (mm)
200
150
100
50
ab
b
a
Developing
Nearly ripe
Post-spawning / recovery
Gonad state

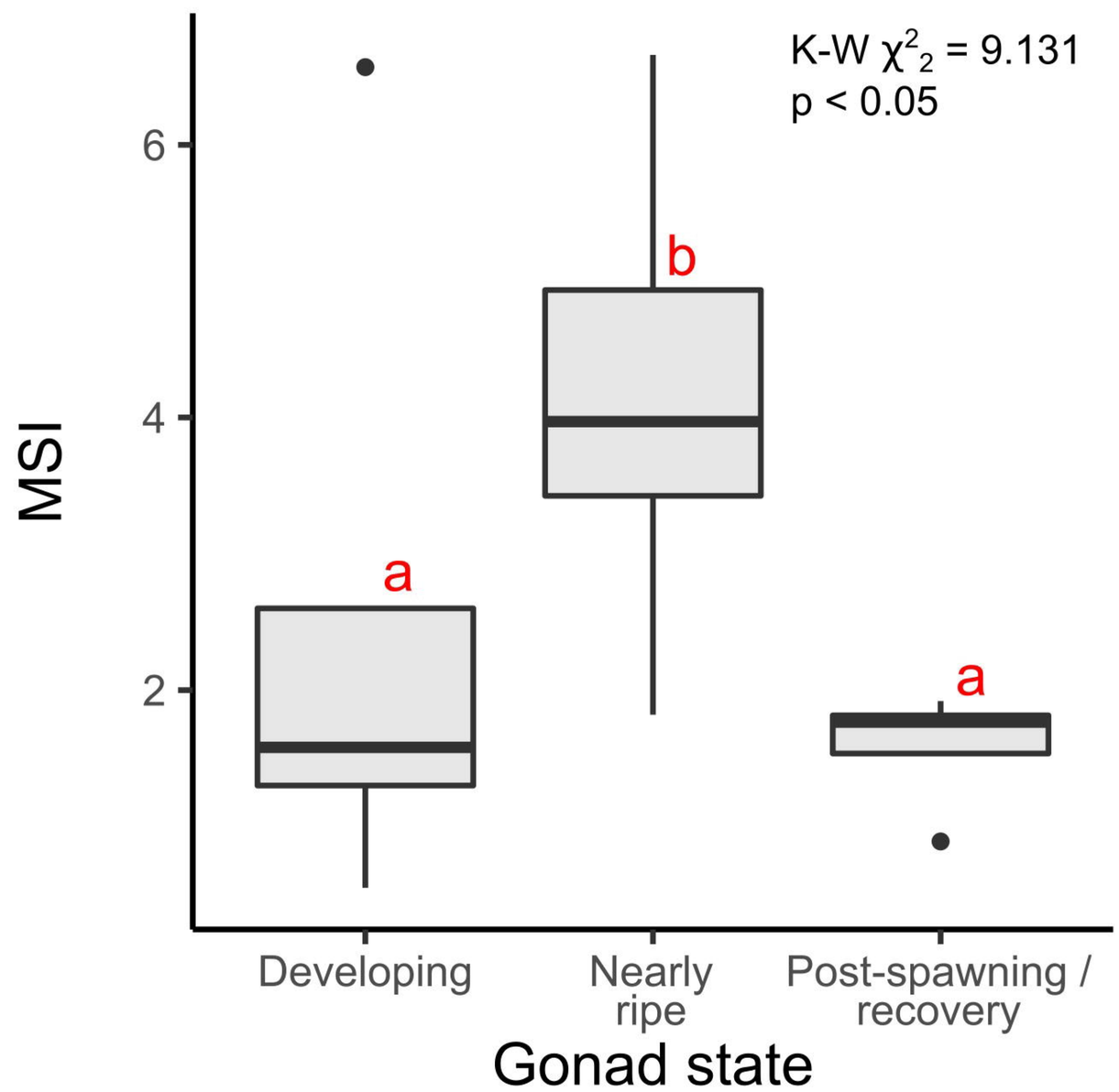
K-W χ^2_2 = 9.131
p < 0.05
MSI
6
4
2
a
b
a
Developing
Nearly ripe
Post-spawning / recovery
Gonad state

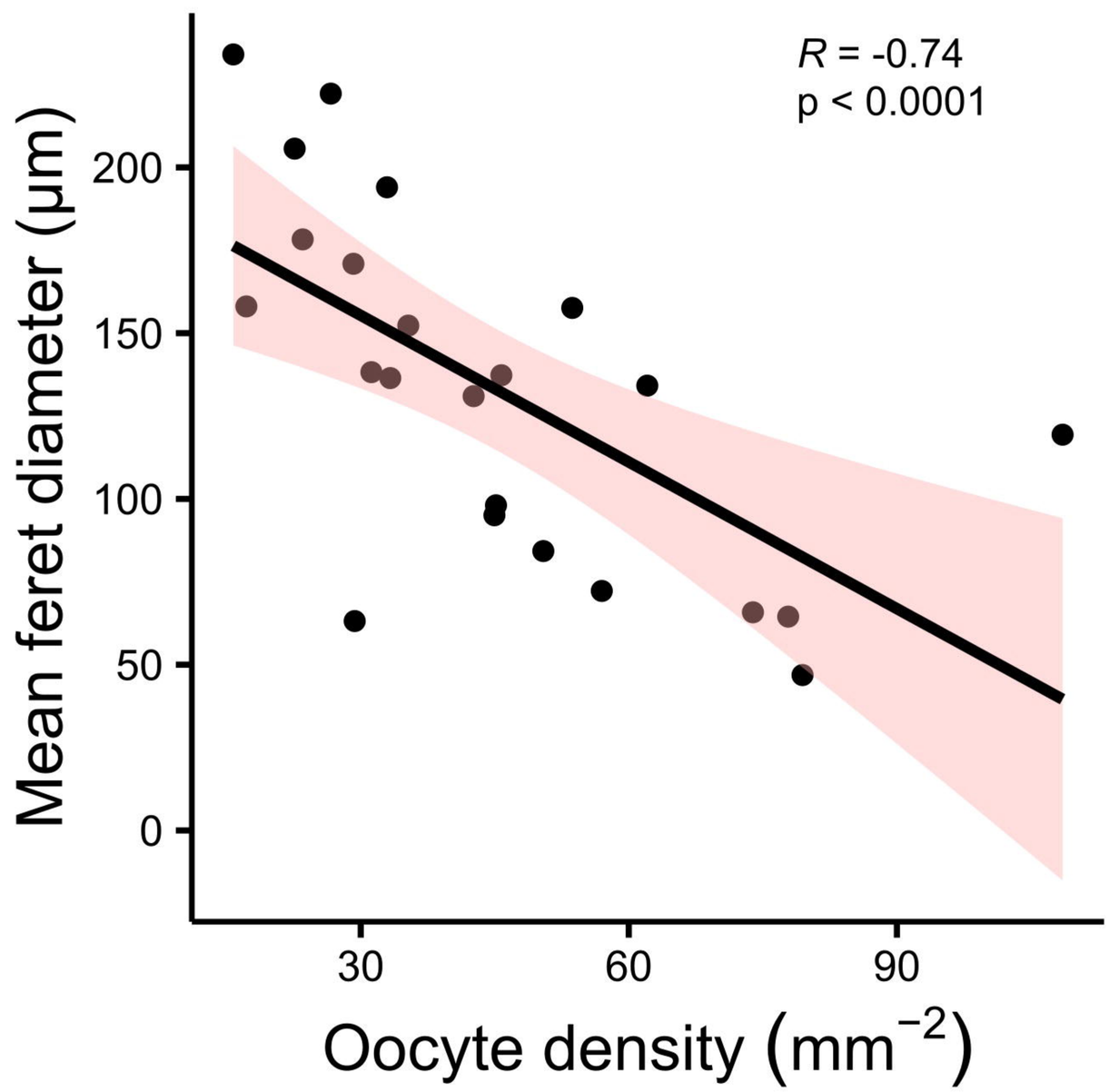
R = -0.74
p < 0.0001
Mean feret diameter (µm)
200
150
100
50
0
30
60
90
Oocyte density (mm^{-2})

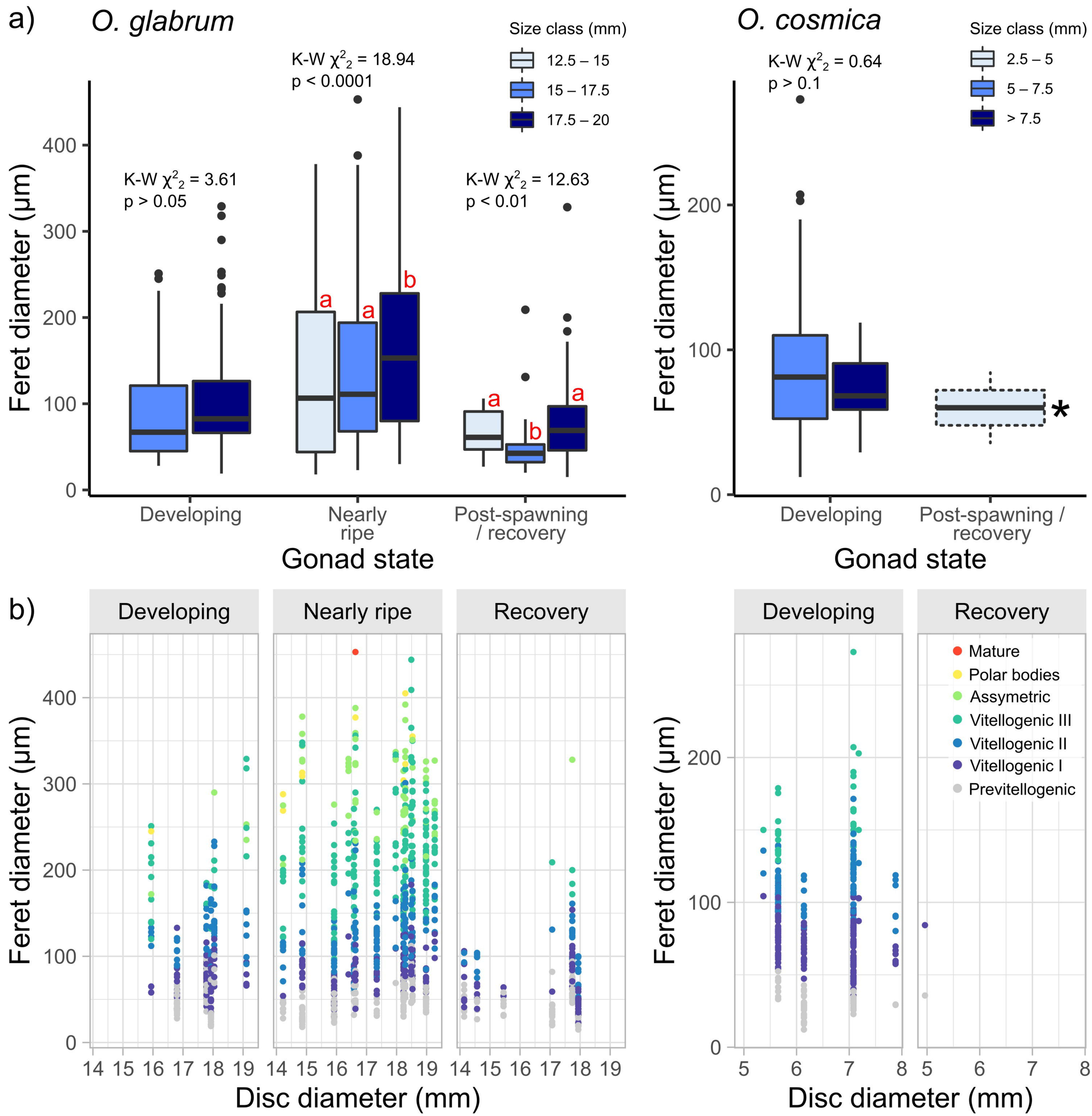
a)
O. glabrum
O. cosmica
Size class (mm)
12.5 – 15
15 – 17.5
17.5 – 20
2.5 – 5
5 – 7.5
> 7.5
K-W χ²₂ = 3.61
p > 0.05
K-W χ²₂ = 18.94
p < 0.0001
K-W χ²₂ = 12.63
p < 0.01
K-W χ²₂ = 0.64
p > 0.1
Feret diameter (µm)
Developing
Nearly ripe
Post-spawning / recovery
Post-spawning / recovery
Gonad state
b)
Developing
Nearly ripe
Recovery
Mature
Polar bodies
Assymetric
Vitellogenic III
Vitellogenic II
Vitellogenic I
Previtellogenic
Disc diameter (mm)